

Nicolette Chahal  
Gleghorn Lab  
9 August 2018

## **Histological Markers of Ventilation-Induced Lung Injury: Implications for Premature Babies**

### **Introduction:**

Preterm birth is defined as a birth that takes place before the 37<sup>th</sup> week of gestation, and is one of the leading causes of neonatal deaths, accounting for 35% of the 3.1 million deaths per year across the globe.<sup>1</sup> Alveolarization, the final stage of lung development, does not start until the 36<sup>th</sup> week of gestation and continues after birth.<sup>1-3</sup> Preterm infants therefore have a lung in saccular stage that results in an inability to adequately exchange gas between the atmosphere and blood. Current treatment involves placing the infant on a ventilator to control respiration and deliver supplemental oxygen to the lungs in order to ensure survival. In term born infants and healthy adults, the body takes in air by contracting the diaphragm and intercostal muscles to expand the thoracic cavity, creating a negative pressure inside cavity.<sup>2</sup> As gases, such as air, flow from high pressure to low pressure, the atmospheric air flows into the lung and gases are exchanged with capillaries in the lung based on diffusion. Mechanical ventilation (MV), however, forces air in by positive pressure, effectively pushing air into the lung, often at non-physiological pressures. This can damage the lungs and creates a high risk for the development of Bronchopulmonary Dysplasia (BPD) in preterm infants.<sup>3,4</sup> Consequences of BPD include an increased risk for respiratory infections and chronic lung disease, which can extend into adulthood, as well as asthma, and pulmonary hypertension.<sup>4</sup> Over the past decade, treatments have been developed that increase the survival rates of premature infants, but none have led to a decline in either the incidence rate of or morbidities associated with BPD. This is due in part to a gap in knowledge of how mechanical forces play a role in alveolarization as well as a lack of effective animal models, which recapitulate all elements of the BPD observed in the clinic.

The ultimate goal of this research is to develop a platform to study the molecular pathways in the lung that are activated during MV and how they contribute to ventilator induced lung injury, thus enabling the development of novel treatments for BPD. Specifically, my project contributes to this goal through developing a method to quantify morphological characteristics of lung tissue. A future direction will be to expand this analysis to tissue exposed to ventilation to analyze and compare MV-induced morphological changes in murine neonate lung tissue to that of healthy lung tissue. To analyze the tissue, histological stains were employed. Specifically, Hematoxylin and Eosin (H&E), Masson's Trichrome, and Verhoeff-Van Gieson (VVG) were utilized to visualize different elements of the lung tissue. H&E stains the nuclei purple and the cytoplasm pink. This stain provides structural information, making it a valuable tool in clinical pathology to identify harmful aspects of tissue, such as tumors and fibrosis. In this study, it will be used to detect changes including inflammation, as well as vascular and alveolar remodeling.

The images obtained from this stain were further analyzed via stereological measurement including quantification of septal volume, mean linear intercept, and the ratio of alveolar volume to lung tissue. The Masson's trichrome stain was used to identify smooth muscle and collagen while VVG was employed to survey elastin fiber networks within the tissue.

In addition to qualitative data drawn from histology, quantitative data will add more concrete evidence of lung injury in the culture model by allowing for in-depth comparisons to be made between injured and healthy tissue harvested from neonate mice at different ages. Stereology is the quantitative analysis of tissue through unbiased sampling and two dimensional measurements that represent the whole organ instead of one image. It is important that the resulting data is in terms of three dimensions because like the body, the lungs and other organs are three dimensional.<sup>5</sup> Quantitative data on lung structure is vital for understanding not only how the lung develops through branching and alveolarization, but also how the alveoli and parenchyma is altered due to a ventilator injury, cancer, or other deformations. One of the most important, and most limiting, aspects of stereology is that the tissue is sampled in an unbiased fashion and is representative of the whole lung. To accomplish this, samples from the tissue must be randomized such that all parts have an equal opportunity to be picked and when collecting data, the researcher must be masked or blinded meaning they cannot have any knowledge of the sample and whether or not it comes from healthy, injured, or treated lung tissue. In this study, we performed estimated septal volume, surface area, and ratio of airspace to interstitium calculations to show that the results from our methods are consistent with what would be expected from a developing lung. These values were chosen because they highlight aspects of the lung that are changed when ventilated. MV causes thickening of the septa, a decrease in alveolar surface area, and an increase of airspace to interstitium, which all contribute to inadequate nutrient exchange between the atmosphere and blood. Future analysis will build on this framework incorporating by assessing other aspects of quantitative lung analysis including air space volume and alveolar surface area as well as comparisons between healthy lung tissue and MV damaged lung tissue of CD1 strained mice.

### **Hypothesis:**

Based on similar experiments performed in other mouse strains, we expect to see an increase in alveolarization and structure with an increase in collagen and elastin development as development progresses. Quantitatively, as the tissue increases in age, the septal volume, surface area, and ratio of airspace to interstitium should also increase. Additionally, in cases of MV, it is expected that a histological analysis will show an increase in septal thickness with enlarged and collapsed alveoli, while a stereological analysis will show an increase in septal volume and airspace with decrease in alveolar surface area.

### **Results:**

Hematoxylin and Eosin (H&E), Masson's Trichrome, and Verhoeff-Van Gieson (VVG) were employed to visualize key elements involved in healthy lung tissue. In H&E stained tissue,

the cytoplasm is stained pink and the nuclei purple (Figure 1A, D). Nuclei in this stain appear as small purple dots highlighted by the black arrow in Figure 1D. This stain is primarily used to analyze structure, morphology, and stereological features. The Masson's trichrome stain depicted in the middle image stains collagen blue, smooth muscle red, and cytoplasm pink. A white arrow is used to highlight collagen, a blue arrow for cytoplasm, and a yellow for smooth muscle (Figure 1E). In the lung, collagen is required; however, in BPD and emphysema there is an over deposition and abnormal arrangement of collagen, causing stiffening of the lung and improper inhalation.<sup>3</sup> It is important to know relative amounts of collagen in the tissue to assist in determining if it is healthy or not. VVG stains elastin blue-black (red arrow), nuclei black (black arrow), and non-specific structures yellow (Figure 1F). Elastin is critical for expansion and deflation during inhalation and exhalation, making it an important characteristic to analyze.<sup>3</sup> Also, basic structures such as alveoli (orange arrow, Figure 1A), major airways (green arrows, Figure 1A and 1B), and vasculature (purple arrow) are critical for accurately analyzing lung tissue.

As mice undergo postnatal growth, the lung also grows in size while the alveoli further branch (septate) to form new alveoli. With the developing lung, septal density, and surface area also increases due to the growing need of exchanging nutrients between the atmosphere and blood. However, the ratio of airspace to interstitium did not follow the predicted trend of increasing airspace as the tissue increases in age (Table 1). This could be due to the fact that when dense lung tissue transitions to areas with larger airspaces, such as P8 lungs, the sample will have more white space (or airspace) in a 2D sample than P14 samples because alveolarization is not as developed. As alveolarization progresses, the alveoli become more branched, but greatly increase in total surface area. Because of this, the ratios of airspace to interstitium in P2 and P14 samples appear similar, but in reality, they are not. Instead of mostly interstitium in the lung, the tissue becomes thinner and denser, creating a larger surface area for maximal gas exchange.

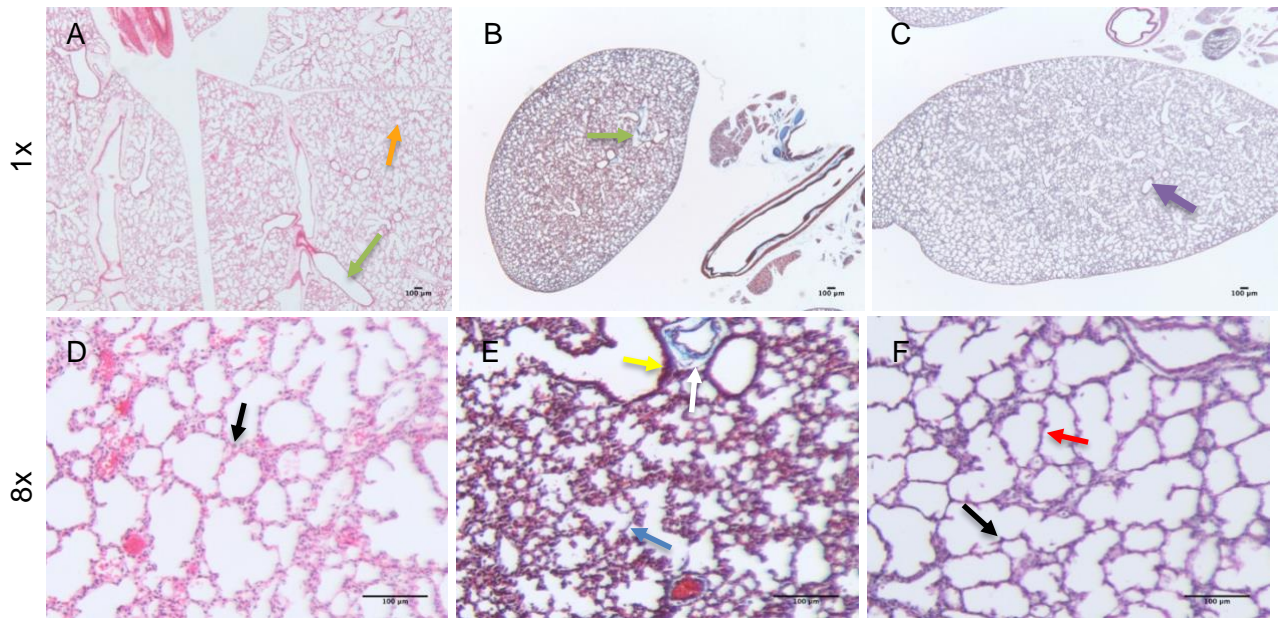


**Figure 1: Histological stains for the assessment of tissue morphology.** H&E sample (A and D), Masson's trichrome (B and E), and VVG samples (C and F) were imaged at 1x and 8x on the Zeiss Discovery.V8 Stereoscope. Arrows on the images highlight different aspects of the tissue including nuclei (black arrows), collagen (white arrow), smooth muscle (yellow arrow), cytoplasm (blue arrow), elastin (red arrow), and structural characteristics such as major airways (green arrows), alveoli (orange arrow), and vasculature (purple arrow). Scale bar is 100 µm.

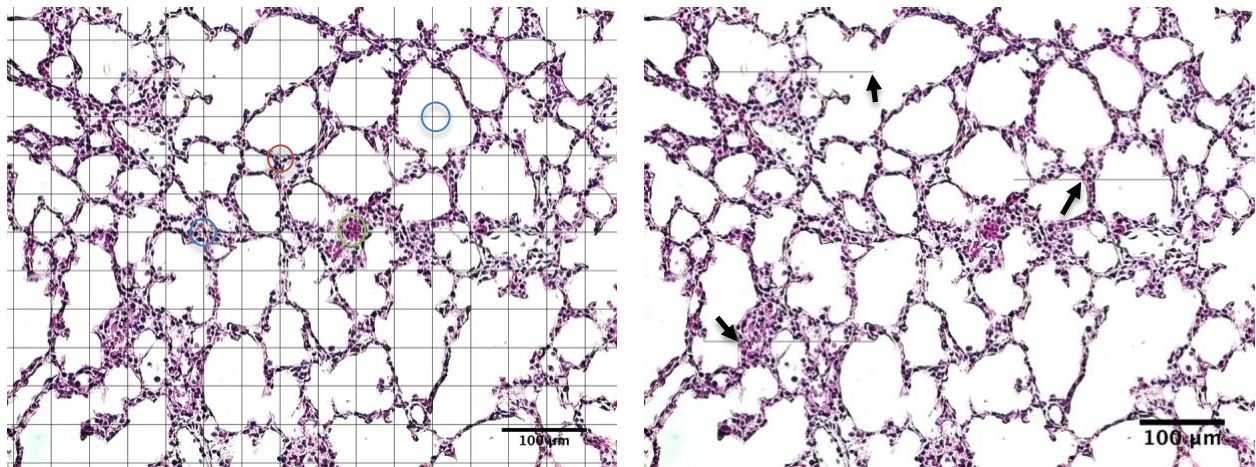


**Figure 2: Septal Volume and Surface Area Stereological Analysis Set-Up.** Examples of the grid and line system to perform a stereological analysis on P8 samples at 20x magnification. The grid on the left represents the point intercept system used to determine the estimated septal ratio volume. For example, the point enclosed by the red circle would be counted as P(septa) while the point enclosed by the blue circles would represent P(parenchyma). Vasculature (green circle) is ignored from this calculation. The image to the right represents the randomly superimposed lines placed on the image to determine the estimated surface area ratio. The black arrows on the lower two test lines indicates to what would be counted as an intersection point while the thicker black arrow on the top points to what would be counted as a reference point. Magnification 20x. Scale bar is 100 µm.

Stereological analysis was performed on 20x magnified H&E stained images by implementing a grid 2000 um apart and imposing 199.37 um long randomized lines (Figure 2). To determine septal volume, the grid was used to count points that intersected with parenchyma and septa, then dividing points of septa by points of parenchyma. To determine alveolar surface area, the randomized lines were used to count total points of reference and intersections of alveolar walls. Then, double the total number of intersections was divided by the distance of the line multiplied by the points of reference.

**Table 1: Stereology results from the H&E stained samples (n=3)**

Age	Septal Density estimation (ratio septa to parenchyma)	Surface Area estimation (ratio alveoli to parenchyma)	Ratio of airspace to interstitium (error: 0.42238)
P2	0.225	0.0333	2.6837
P8	0.309	0.0424	2.9972
P14	0.645	0.0721	1.7675

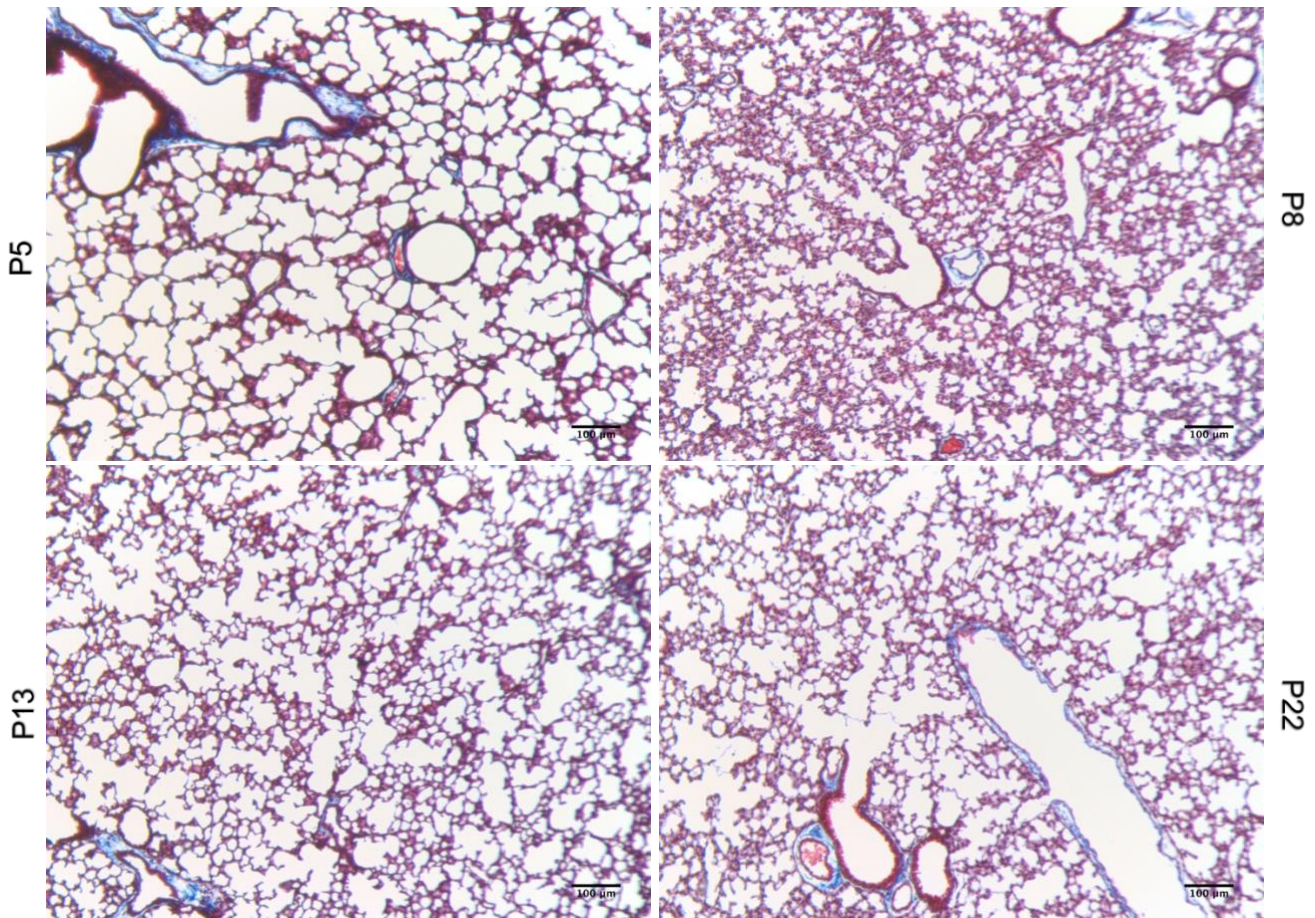


**Figure 3: Masson's trichrome stained neonate mice from the ages of P5 to P22.** Nuclei are colored black, collagen blue, and cytoplasm/muscle red. P5, P8, P13, and P22 lungs show expected alveolarization and branching. Also, an increase in collagen is noted with the increasing age, especially around major airways and vasculature. Magnification 20x. Scale bar is 100 µm.

Neonatal lung tissue from P5, P8, P13, and P22 were stained with a Masson's trichrome to visualize alveolarization and collagen deposition. It was observed that as the mice grow older, there is more branching and alveolarization, but also more collagen present in the tissue. This shows that with age, the lungs become more developed and structurally stable. Collagen is required in the lung to hold structure and geometry of the parenchyma and aid in the function of the lung (Figure 3).

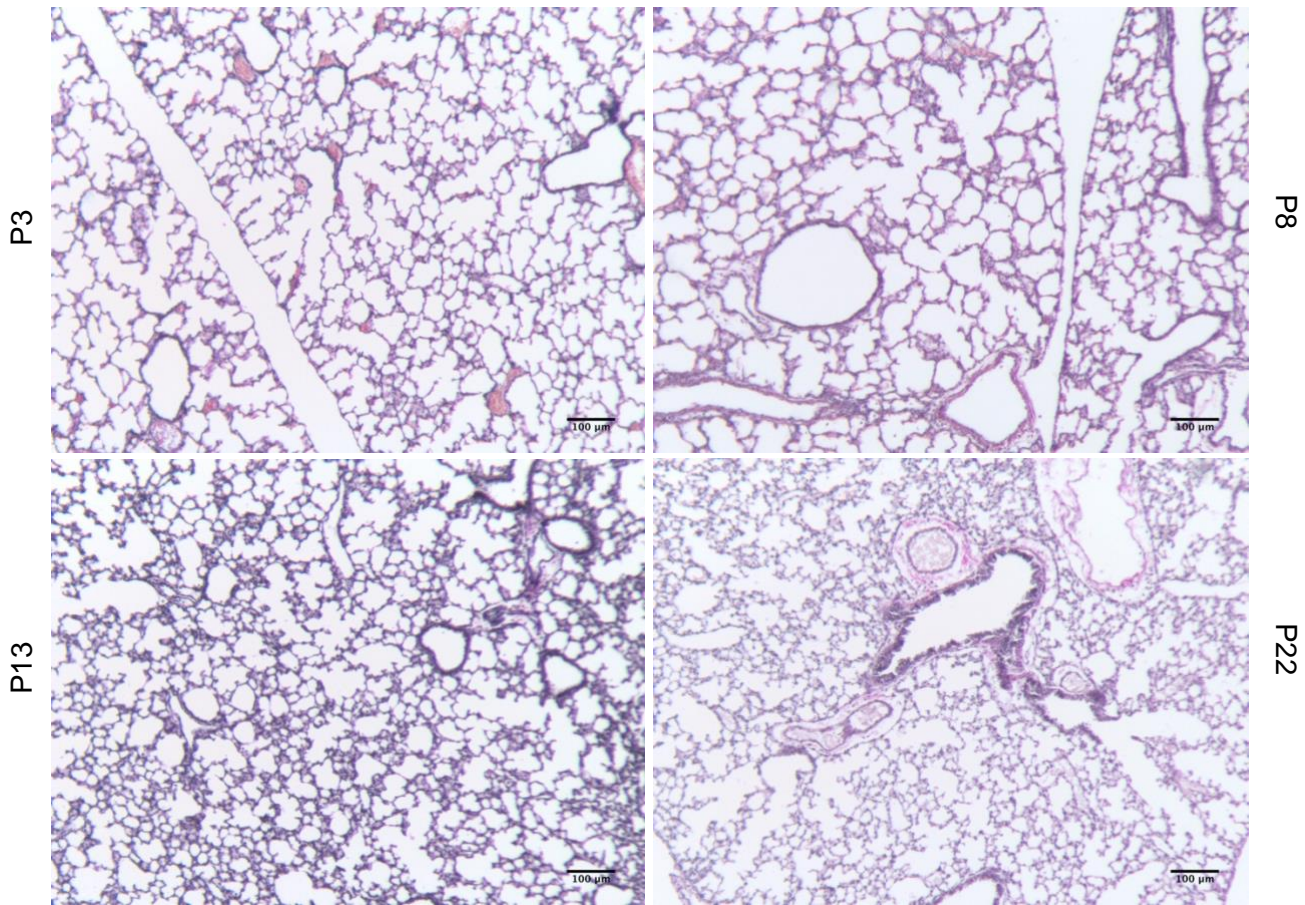


**Figure 4: Verhoeff Van-Gieson stained neonatal lung tissue ranging from the age of P3 to P22.** The Van-Gieson stain stains elastin blue-black (or purple in this case), nuclei black, collagen red, and non-specific structures, such as blood, yellow. P2, P4, P13, and P22 show expected alveolarization and parenchyma complexity. Also, there is a higher concentration of elastin during alveolarization (P13). Magnification 20x. Scale bar is 100 μm.

Neonatal tissue from P3, P8, P13, and P22 were stained with a Verhoeff Van-Gieson stain to visualize alveolarization and elastin (Figure 4). As age increases, alveoli are seen branching and becoming denser in the lobe, which is in agreement with both the H&E and Masson's trichrome stains. Elastin allows the lung to stretch during inhalation and then return to its natural state without damage during exhalation. Seen in the pictures above, every alveoli and branch are lined purple, indicating there is elastin present.<sup>3</sup> Throughout all stages, elastin is remodeling and constantly present. The difference in shade between P13 and P22 could account for an increase in elastin during alveolarization, which has ended by P22. (Figure 4).

#### **Limitations and Future directions:**

As we did not have previous experience with stereological analysis, I developed the protocols and methods adapting and borrowing heavily from the literature. Starting with a new litter of mice, there will be new protocols in place so that the researcher performing the stereological analysis has no knowledge on age, breed, or conditions of the tissue samples (i.e. is masked). Additionally, creating a set method of how many samples should be included,

differentiating between septal tissue and alveolar wall, and eliminating vasculature will need to be refined. Furthermore, fixations will also have to be constant due to blood in the lung impacting stereological measurements by making it hard to see a clear difference in septa and parenchyma. Once a set method is in place for quantitative lung analysis using stereology, the next step will be to analyze mechanically ventilated tissue to compare to the healthy samples described above.

### **Materials and methods:**

Dissections: P5-P22 CD1 mice were obtained from the Animal Facility at the University of Delaware and underwent euthanasia with an IP injection of sodium pentobarbital. Mice were weighed and placed under a stereo microscope. Toe pinch was performed to ensure a non-response. After confirming euthanasia, the abdominal and thoracic cavities were cut open and the ribs cut back to expose the heart. A 4% wt/vol sodium citrate perfusion was then performed at a pressure of 10-15 cmH<sub>2</sub>O for 5 minutes by cannulating the right ventricle with a beveled needle. Next, the lung in the thoracic cavity was exposed by cutting the ribs along the midline and the trachea exposed by removing soft tissue from the neck. Then, the esophagus was cut behind the liver and the trachea cut near the pharynx. After freeing these structures from surrounding connective tissue, the lungs, heart, and trachea were removed *en bloc*. The lungs were then placed in an ex vivo culture device made from PBS and Dent's or PFA fixative perfusion was performed through the trachea at a pressure of 20 cm H<sub>2</sub>O for 10 minutes. Next, a fixative perfusion was performed on the right ventricle for 5 minutes at 10 cm H<sub>2</sub>O. Finally, the lung was stored in the fixative in the 4°C fridge overnight.

Processing, embedding, and paraffin sectioning: After the samples were removed from the 4°C fridge, they were placed in designated cassettes (whole, lobe, or fragment) and labeled. Then, they were processed into paraffin in a Miles Scientific Tissue Tech VP tissue processor overnight. When finished, the samples were taken out of the processor and immediately embedded in paraffin using a Tissue Tek tissue embedding stations. Once embedded in paraffin blocks, the samples were then sectioned at an 11 degree angle at 7 um thick and baked overnight at 37°C. The next morning the slides were baked for an additional 90 minutes at 60°C.

Staining: All staining processes began with a basic deparaffinization of the slides. For the H&E protocol, the slides were stained with Meyer's Hematoxylin for 8 minutes and put under a running tap for 6 minutes. Next, the slides were dipped in distilled water and 95% ethanol 10 times each, then placed in Eosin Y for exactly 1 minute and 15 seconds. The tissue on the slides was then hydrated and cover slipped. Masson's trichrome staining was performed by first dipping the slides in DI water 20 times and then placing it in Bouin's fixative for 12 hours. After, the slides were placed under running tap water (10 minutes), dipped in DI water 20 times, and then placed in Weigart's Iron Hematoxylin (3 minutes). The slides were placed under another running tap for 8 minutes and then dipped in DI water 20 times. Next, the slides were placed in

Biebrich Scarlet-Acid Fuchsin (10 minutes), dipped in DI water, placed in Phosphomolybdic:phosphotungstic Acid (8 minutes), and Aniline Blue (3 minutes) before being dipped in DI water. Finally, the slides were placed in 1% Acetic Acid Solution (5 minutes) and dipped in DI water before being hydrated and cover slipped. The VVG stain protocol was performed according to IHCworld.com and the only deviation was the slides were kept in the Verhoeff's Working solution for 45 minutes instead of 1 hour.

Imaging: Slides stained with H&E were imaged on the microscope Zeiss Imager.A2 Upright Epifluorescence microscope using Axiovision SE64 to capture the images. For the slides stained with Masson's trichrome and VVG, the Zeiss Stereoscope with an Axio ERc5s camera and Live czi-Zen 23 program was used to image. To avoid biased, a random number generator was used to pick the slide in the group that was being imaged. For example, slides 1576-1616 represented H&E stained P8 samples. Using Google's random number generator, slide 1590 was selected and then imaged. Furthermore, each slide was imaged at the same general area: the second sample towards the middle right of the tissue.

Stereology/Imaging Processing: To determine the septal volume, a basic point system was created with a random grid fixated on the image 2000 um apart and the sum of the points that hit the septal tissue was divided by the sum of the points that hit parenchyma.<sup>6,7</sup> The surface area density was determined by superimposing three 199.37 um lines onto the picture by breaking the image into six blocks and using a random number generator to determine what box the line would be placed in. Tissue that was less than 20 um was counted as septa while anything 20 um and over along with airspace was counted as parenchyma. Next, the data collected from the image was used to determine the estimated surface area following basic protocols.<sup>8</sup> Finally, the ratio of airspace to interstitium was determined using a custom MATLAB script. In short, the vasculature was converted to be the same color as the tissue, a binary image created, and then a ratio of the number of white pixels to black pixels measured.

### **Acknowledgements:**

Funding for this work was provided, in part, by the University of Delaware Undergraduate Research Program. Also, I would like to thank everyone at the Gleghorn lab, specifically Dr. Gleghorn, Rob McKee, and Mary Athansopoulos for helping me develop skills in the lab and starting up my first project.

## References:

1. Kumar V. Diagnostic Approach to Pulmonary Hypertension in Premature Neonates. *Children*. 2017;4(9):75. doi:10.3390/children4090075.
2. Schöni-Affolter F, Dubuis-Grieder C, Strauch E. 18.1 Phases of lung development. *embryology.ch*. <http://www.embryology.ch/anglais/rrespiratory/phases01.html>. Accessed August 8, 2018.
3. Jobe AJ. The New BPD: An Arrest of Lung Development. *Pediatric Research*. 1999;46(6):641-641. doi:10.1203/00006450-199912000-00007.
4. Carvalho CG, Silveira RC, Procianoy RS. Ventilator-induced lung injury in preterm infants. *Revista Brasileira de Terapia Intensiva*. 2013;25(4). doi:10.5935/0103-507x.20130054.
5. Ochs M, Mühlfeld C. Quantitative microscopy of the lung: a problem-based approach. Part 1: basic principles of lung stereology. *American Journal of Physiology-Lung Cellular and Molecular Physiology*. 2013;305(1):L15-L22. doi:10.1152/ajplung.00429.2012.
6. Hsia CCW, Hyde DM, Ochs M, Weibel ER. An Official Research Policy Statement of the American Thoracic Society/European Respiratory Society: Standards for Quantitative Assessment of Lung Structure. *American Journal of Respiratory and Critical Care Medicine*. 2010;181(4):394-418. doi:10.1164/rccm.200809-1522st.
7. Pieretti AC, Ahmed AM, Roberts JD, Kellher CM. A novel in vitro model to study alveologensis. *American Journal of Respiratory Cell and Molecular Biology*. 2014;50(2):459-469. doi:10.1165/rcmb.2013-0056OC.
8. Schneider JP, Ochs M. Chapter 12 - Stereology of the Lung. *Methods in Cell Biology*. 2013;113:257-294. doi:10.1016/B978-0-12-407239-8.00012-4.